References

1. Taub R. Liver regeneration 4: transcriptional control of liver regeneration. FASEB J 1996;10:413-427.
2. Fausto N. Liver regeneration. J Hepatol 2000;32:19-31.
3. McMahon JB, Richards WL, de Campo AA, Song MK, Thorgeirsson SS. Differential effects of transforming growth factor-beta on proliferation of normal and malignant rat liver epithelial cells in culture. Cancer Res 1986;46:4665-4671.
4. Michalopoulos GK. Liver regeneration. J Cell Physiol 2007;213: 286-300.
5. Jakowlew SB, Mead JE, Danielpour D, Wu J, Roberts AB, Fausto N. Transforming growth factor-beta (TGF-beta) isoforms in rat liver regeneration: messenger RNA expression and activation of latent TGF-beta. Cell Regul 1991;2:535-548.
6. Braun L, Mead JE, Panzica M, Mikumo R, Bell GI, Fausto N. Transforming growth factor beta mRNA increases during liver regeneration: a possible paracrine mechanism of growth regulation. Proc Natl Acad Sci U S A 1988;85:1539-1543.
7. Oe S, Lemmer ER, Conner EA, Factor VM, Levéen P, Larsson J, et al. Intact signaling by transforming growth factor beta is not required for termination of liver regeneration in mice. Hepatology 2004;40: 1098-1105.
8. Mosher DF. Physiology of thrombospondin. Annu Rev Med 1990;41: 85-97.
9. Crawford SE, Stellmach V, Murphy-Ullrich JE, Ribeiro SM, Lawler J, Hynes RO, et al. Thrombospondin-1 is a major activator of TGF-beta1 *in vivo*. Cell 1998;93:1159-1170.
10. Adams JC. Thrombospondins: multifunctional regulators of cell interactions. Annu Rev Cell Dev Biol 2001;17:25-51.
11. Kyriakides TR, Maclauchlan S. The role of thrombospondins in wound healing, ischemia, and the foreign body reaction. J Cell Commun Signal 2009;3:215-225.
12. Lawler J, Sunday M, Thibert V, Duquette M, George EL, Rayburn H, Hynes RO. Thrombospondin-1 is required for normal murine pulmonary homeostasis and its absence causes pneumonia. J Clin Invest 1998;101:982-992.
13. Moriya K, Bae E, Honda K, Sakai K, Sakaguchi T, Tsujimoto I, et al. A fibronectin-independent mechanism of collagen fibrillogenesis in adult liver remodeling. Gastroenterology 2011;140:1653-1663.
14. Yuan H, Zhang H, Wu X, Zhang Z, Du D, Zhou S, et al. Hepatocyte-specific deletion of Cdc42 results in delayed liver regeneration after partial hepatectomy in mice. Hepatology 2009;49:240-249.
15. Yoshie M, Nishimori H, Lee GH, Ogawa K. High colony forming capacity of primary cultured hepatocytes as a dominant trait in hepatocarcinogenesis-susceptible and resistant mouse strains. Carcinogenesis 1998;19:1103-1107.
16. Ribeiro SM, Poczatek M, Schultz-Cherry S, Villain M, Murphy-Ullrich JE. The activation sequence of thrombospondin-1 interacts with the latency-associated peptide to regulate activation of latent transforming growth factor-beta. J Biol Chem 1999;274:13586-13593.
17. Meek RL, Cooney SK, Flynn SD, Chouinard RF, Poczatek MH, Murphy-Ullrich JE, Tuttle KR. Amino acids induce indicators of response to injury in glomerular mesangial cells. Am J Physiol Renal Physiol 2003;285:F79-F86.
18. Asai K, Tamakawa S, Yamamoto M, Yoshie M, Tokusashi Y, Yaginuma Y, et al. Activated hepatic stellate cells overexpress p75NTR after partial hepatectomy and undergo apoptosis on nerve growth factor stimulation. Liver Int 2006;26:595-603.
19. Breitkopf K, Sawitza I, Westhoff JH, Wickert L, Dooley S, Gressner AM. Thrombospondin 1 acts as a strong promoter of transforming growth factor beta effects via two distinct mechanisms in hepatic stellate cells. Gut 2005;54:673-681.
20. Albrecht JH, Poon RYC, Ahonen CL, Rieland BM, Deng C, Crary GS. Involvement of p21 and p27 in the regulation of CDK activity and cell cycle progression in the regenerating liver. Oncogene 1998;16: 2141-2150.
21. Westerhausen DR, Jr, Hopkins WE, Billadello JJ. Multiple transforming growth factor-beta-inducible elements regulate expression of the plasminogen activator inhibitor type-1 gene in Hep G2 cells. J Biol Chem 1991;266:1092-1100.
22. Lee FY, Li Y, Zhu H, Yang S, Lin HZ, Trush M, Diehl AM. Tumor necrosis factor increases mitochondrial oxidant production and induces expression of uncoupling protein-2 in the regenerating mice [correction of rat] liver. Hepatology 1999;29:677-687.
23. Kaur S, Martin-Manso G, Pendrak ML, Garfield SH, Isenberg JS, Roberts DD. Thrombospondin-1 inhibits VEGF receptor-2 signaling by disrupting its association with CD47. J Biol Chem 2010;285: 38923-38932.
24. Taub R. Liver regeneration: from myth to mechanism. Nat Rev Mol Cell Biol 2004;5:836-847.
25. Nakatani T, Inouye M, Mirochnitchenko O. Overexpression of antioxidant enzymes in transgenic mice decreases cellular ploidy during liver regeneration. Exp Cell Res 1997;236:137-146.
26. Tomomura A, Sawada N, Sattler GL, Kleinman HK, Pitot HC. The control of DNA synthesis in primary cultures of hepatocytes from adult and young rats: interactions of extracellular matrix components, epidermal growth factor, and the cell cycle. J Cell Physiol 1987;130:221-227.
27. Ning M, Sarracino DA, Kho AT, Guo S, Lee SR, Krastins B, et al. Proteomic temporal profile of human brain endothelium after oxidative stress. Stroke 2011;42:37-43.
28. Ding BS, Nolan DJ, Butler JM, James D, Babazadeh AO, Rosenwaks Z, et al. Inductive angiocrine signals from sinusoidal endothelium are required for liver regeneration. Nature 2010;468:310-315.
29. Zhang X, Lawler J. Thrombospondin-based antiangiogenic therapy. Microvasc Res 2007;74:90-99.
30. Albrecht JH, Meyer AH, Hu MY. Regulation of cyclin-dependent kinase inhibitor p21(WAF1/Cip1/Sdi1) gene expression in hepatic regeneration. Hepatology 1997;25:557-563.
31. Annes JP, Munger JS, Rifkin DB. Making sense of latent TGFbeta activation. J Cell Sci 2003;116:217-224.
32. Shimizu M, Hara A, Okuno M, Matsuno H, Okada K, Ueshima S, et al. Mechanism of retarded liver regeneration in plasminogen activator-deficient mice: impaired activation of hepatocyte growth factor after Fas-mediated massive hepatic apoptosis. Hepatology 2001;33: 569-576.
33. Chen RH, Su YH, Chuang RL, Chang TY. Suppression of transforming growth factor-beta-induced apoptosis through a phosphatidylinositol 3-kinase/Akt-dependent pathway. Oncogene 1998;17: 1959-1968.
34. Chen RH, Chang MC, Su YH, Tsai YT, Kuo ML. Interleukin-6 inhibits transforming growth factor-beta-induced apoptosis through the phosphatidylinositol 3-kinase/Akt and signal transducers and activators of transcription 3 pathways. J Biol Chem 1999;274: 23013-23019.
35. Sun J, Hopkins BD, Tsujikawa K, Perruzzi C, Adini I, Swerlick R, et al. Thrombospondin-1 modulates VEGF-A-mediated Akt signaling and capillary survival in the developing retina. Am J Physiol Heart Circ Physiol 2009;296:H1344-H1351.
36. Wang Y, Wang S, Sheibani N. Enhanced proangiogenic signaling in thrombospondin-1-deficient retinal endothelial cells. Microvasc Res 2006;71:143-151.

Published OnlineFirst May 2, 2012; DOI:10.1158/0008-5472.CAN-12-0299

Cancer Research

CD44s Regulates the TGF-β–Mediated Mesenchymal Phenotype and Is Associated with Poor Prognosis in Patients with Hepatocellular Carcinoma

Kosuke Mima, Hirohisa Okabe, Takatsugu Ishimoto, et al.

Cancer Res 2012;72:3414-3423. Published OnlineFirst May 2, 2012.

Published OnlineFirst May 2, 2012; DOI:10.1158/0008-5472.CAN-12-0299

CD44s Regulates the TGF-β–Mediated Mesenchymal Phenotype and Is Associated with Poor Prognosis in Patients with Hepatocellular Carcinoma

Kosuke Mima[1], Hirohisa Okabe[1], Takatsugu Ishimoto[1], Hiromitsu Hayashi[1], Shigeki Nakagawa[1], Hideyuki Kuroki[1], Masayuki Watanabe[1], Toru Beppu[1], Mayumi Tamada[2], Osamu Nagano[2], Hideyuki Saya[2], and Hideo Baba[1]

Abstract

The prognosis for individuals diagnosed with hepatocellular carcinoma (HCC) remains poor because of the high frequency of invasive tumor growth, intrahepatic spread, and extrahepatic metastasis. Here, we investigated the role of the standard isoform of CD44 (CD44s), a major adhesion molecule of the extracellular matrix and a cancer stem cell marker, in the TGF-β–mediated mesenchymal phenotype of HCC. We found that CD44s was the dominant form of CD44 mRNA expressed in HCC cells. Overexpression of CD44s promoted tumor invasiveness and increased the expression of vimentin, a mesenchymal marker, in HCC cells. Loss of CD44s abrogated these changes. Also in the setting of CD44s overexpression, treatment with TGF-β1 induced the mesenchymal phenotype of HCC cells, which was characterized by low E-cadherin and high vimentin expression. Loss of CD44s inhibited TGF-β–mediated vimentin expression, mesenchymal spindle-like morphology, and tumor invasiveness. Clinically, overexpression of CD44s was associated with low expression of E-cadherin, high expression of vimentin, a high percentage of phospho-Smad2–positive nuclei, and poor prognosis in HCC patients, including reduced disease-free and overall survival. Together, our findings suggest that CD44s plays a critical role in the TGF-β–mediated mesenchymal phenotype and therefore represents a potential therapeutic target for HCC. *Cancer Res; 72(13); 3414–23. ©2012 AACR.*

Introduction

Hepatocellular carcinoma (HCC) is the fifth most prevalent and the third most deadly type of cancer worldwide. In fact, it is diagnosed in more than half a million people worldwide each year (1). Surgical resection and liver transplantation are available options for the treatment of early-stage HCC; however, the prognosis of HCC remains poor because of a high level of tumor invasiveness, frequent intrahepatic spread, extrahepatic metastasis, and resistance to chemotherapy (2).

Epithelial–mesenchymal transition (EMT) has been shown to be a pivotal mechanism contributing to cancer invasion and metastasis including HCC (3–7) because epithelial cells lose their polarity and acquire the migratory properties of mesenchymal cells in the developmental process. In recent metastasis researches, EMT is also shown to play an important role in stem-like properties (8).

CD44, a major adhesion molecule of the extracellular matrix, has been implicated in a wide variety of physiologic processes, including leukocyte homing and activation, wound healing, and cell migration (9, 10). Cells produce CD44 protein isoforms through the process of alternative mRNA splicing. The CD44 standard isoform (CD44s) is expressed predominantly in hematopoietic cells and normal epithelial cell subsets, whereas the variant isoform (CD44v) is expressed by some epithelial cells during embryonic development, during lymphocyte maturation and activation, and by several types of carcinoma cells. Recently, cancer stem cells (CSC) in many tumors have been identified by positive expression of CD44, either individually or in combination with other markers, and these cells have been shown to be involved in tumor progression and metastasis (10–16). Although TGF-β signaling is a major regulator of EMT and it maintains the mesenchymal phenotype and stem cell states in an autocrine fashion in cancer (17), the underlying molecular mechanisms that integrate the mesenchymal phenotype with the EMT process and with CSC properties still remain unknown. Therefore, we hypothesize that CD44, a CSC marker, plays an important role in inducing EMT or in maintaining the mesenchymal phenotype in HCC.

Authors' Affiliations: [1]Department of Gastroenterological Surgery, Graduate School of Medical Sciences, Kumamoto University, Honjo, Kumamoto; and [2]Division of Gene Regulation, Institute for Advanced Medical Research, School of Medicine, Keio University, Shinanomachi, Shinjuku-ku, Tokyo, Japan

Note: Supplementary data for this article are available at Cancer Research Online (http://cancerres.aacrjournals.org/).

Corresponding Author: Hideo Baba, Department of Gastroenterological Surgery, Graduate School of Medical Sciences, Kumamoto University, 1-1-1 Honjo, Kumamoto 860-8556, Japan. Phone: 81-96-373-5212; Fax: 81-96-371-4378; E-mail: hdobaba@kumamoto-u.ac.jp

doi: 10.1158/0008-5472.CAN-12-0299

Published OnlineFirst May 2, 2012; DOI:10.1158/0008-5472.CAN-12-0299

Materials and Methods

Cell lines, culture conditions, and reagents

The human HCC lines PLC/PRF/5, HuH1, HLF, and HLE were purchased from the Japanese Collection of Research Bioresources. SK HEP-1 cells were purchased from American Type Culture Collection. The cells were routinely maintained in Dulbecco's Modified Eagle's Medium (Invitrogen) supplemented with 10% FBS (Invitrogen). The cells were incubated at 37°C in a 5% CO_2 air-humidified atmosphere. Purified recombinant human TGF-β1 (R&D Systems) was reconstituted in sterile 4 mmol/L HCl containing 1 mg/mL bovine serum albumin (Sigma). TGF-β1 was used at the indicated concentrations in serum-free medium.

Plasmids and siRNA transfection

The cDNA corresponding to human CD44s was introduced into the pcDNA3.1 expression plasmid (Invitrogen; ref. 18). PLC/PRF/5 cells were transfected with the resulting plasmids using Lipofectamine 2000 (Invitrogen). CD44 expression was transiently downregulated using a predesigned siRNA duplex directed against CD44, and a nontargeting siRNA was used as a negative control. The sequences of the siRNA (chimeric RNA–DNA) duplexes (Japan Bioservice) were as follows (18): CD44 siRNA, 5′-AAAUGGUCGCUACAGCAUCTT-3′ and 5′-GAUGCUGUAGCGACCAUUUTT-3′, and control siRNA, 5′-CGUACGCGGAAUACUUCGATT-3′ and 5′-UCGAAGUAUUCCGCGUACGTT-3′. HCC cells were transfected with the annealed siRNA for 24 to 72 hours using Lipofectamine 2000.

Protein extraction and Western blot analysis

Protein extraction from cultivated cells and Western blot analyses were carried out as previously described (19, 20). Briefly, the cells were lysed in cell lysis buffer containing 25 mmol/L Tris (pH 7.4), 100 mmol/L NaCl, and 1% Tween 20. Equal amount of proteins were loaded onto 10% gels and separated using SDS-PAGE. The resolved proteins were electrophoretically transferred to polyvinylidene fluoride membranes (Bio-Rad, Inc.). The membranes were blocked with 5% low-fat dry milk in TBS-T [25 mmol/L Tris (pH 7.4), 125 mmol/L NaCl, 0.4% Tween 20] for 1 hour at room temperature, followed by incubation with a primary antibody at 4°C overnight. The blots were extensively washed with TBS-T and incubated with an horseradish peroxidase (HRP)-conjugated secondary antibody diluted 1:2,000 in TBS-T for 1 hour at room temperature. The membranes were washed and visualized using a Chemiluminescent Detection Reagent Kit (ECL; GE Healthcare Corp.). Primary antibodies for E-cadherin (1:1,000 dilution; BD Transduction Laboratories), vimentin (1:1,000 dilution; Santa Cruz), CD44s (1:1,000 dilution; Bender MedSystems), phospho-Smad2 (1:500 dilution; Cell Signaling), Smad2/3 (1:1,000 dilution; Cell Signaling), and β-actin (1:1,000 dilution; Cell Signaling) were used for this study.

RNA extraction and quantitative reverse transcription PCR

Total RNA extraction, cDNA synthesis, and quantitative reverse transcription PCR (qRT-PCR) were carried out as previously described (19, 20). Total cellular RNA was extracted using the RNeasy Mini Kit (Qiagen), and cDNA was synthesized with the SuperScript III Transcriptor First Strand cDNA Synthesis System for RT-PCR (Invitrogen) according to the manufacturers' instructions. qRT-PCR was carried out using a LightCycler 480 II instrument (Roche). To determine the differences in the gene expression levels between specimens, the $2^{-\Delta\Delta C_t}$ method was used to measure the fold changes among the samples (21). To carry out qRT-PCR, primers were designed using the Universal Probe Library (Roche) following the manufacturer's recommendations. The primer sequences and probes used for real-time PCR were as follows: E-cadherin, 5′-TTGACGCCGAGAGCTACAC-3′, 5′-GTCGACCGGTGCAATCTT-3′, and universal probe #80; vimentin, 5′-TACAGGAAGCTGCTGGAAGG-3′, 5′-ACCAGAGGGAGTGAATCCAG-3′, and universal probe #13; CD44, 5′-GCAGTCAACAGTCGAAGAAGG-3′, 5′-TGTCCTCCACAGCTCCATT-3′, and universal probe #29; glyceraldehyde-3-phosphate dehydrogenase (GAPDH), 5′-AGCCACATCGCTCAGACAC-3′, 5′-GCCCAATACGACCAAATCC-3′, and universal probe #60; EpCAM, 5′-AGTTGGTGCACAAAATACTGTCAT-3′, 5′-TCCCAAGTTTTGAGCCATTC-3′, and universal probe #8; CD133, 5′-TCCACAGAAATTTACCTACATTGG-3′, 5′-CAGCAGAGAGCAGATGACCA-3′, and universal probe #83; Bmi1, 5′-TTCTTTGACCAGAACAGATTGG-3′, 5′-GCATCACAGTCATTGCTGCT-3′, and universal probe #63; CD13, 5′-TTGCCTACCAGAACACCATCT-3′, 5′-GTTGGATGGACCGGTTGTT-3′, and universal probe #75; and CD90, 5′-CAGAACGTCACAGTGCTCAGA-3′, 5′-GAGGAGGGAGAGGGAGAGC-3′, and universal probe #66. To analyze the CD44 splice variants in human HCC cell lines, the following human primer sets (forward and reverse, respectively) were used: CD44, 5′-TCCCAGACGAAGACAGTCCCTGGAT-3′ and 5′-CACTGGGGTGGAATGTGTCTTGGTC-3′, and GAPDH, 5′-AGCCACATCGCTCAGACAC-3′ and 5′-GCCCAATACGACCAAATCC-3′.

Invasion assay

An *in vitro* cell invasion assay was done as previously described (20). Briefly, the invasion rate of tumor cells that migrated through transwell inserts (8-μm pore size) with a uniform layer of BD Matrigel basement membrane matrix (BD Biosciences) was assessed according to the manufacturer's recommended protocol. The cells were seeded (5×10^4) in 500 μL of serum-free medium into the upper chamber of the insert, and medium containing 10% FBS was added to the lower chamber. After 22 hours, the noninvading cells were removed with a cotton swab, and the invading cells were stained with 1% toluidine blue and counted under a microscope.

Patients and treatment

Among the 235 consecutive patients who had undergone curative hepatic resection between 2004 and 2007 in the Department of Gastroenterological Surgery, Graduate School of Medical Sciences, Kumamoto University, 150 primary HCC samples were analyzed in this study. None of the patients received any preoperative anticancer treatment. The pathologic diagnoses and the clinicopathologic

Published OnlineFirst May 2, 2012; DOI:10.1158/0008-5472.CAN-12-0299

factors were established based on the general guideline for primary liver cancer as defined by the Liver Cancer Study Group of Japan (22, 23) and the American Joint Committee on Cancer (AJCC)/International Union Against Cancer (UICC) staging system (24). The median follow-up duration after surgery was 44 months. This study was approved by the Human Ethics Review Committee of the Graduate School of Medicine, Kumamoto University (Kumamoto, Japan).

Immunohistochemistry and scoring

The sample processing and immunohistochemistry (IHC) procedures were carried out as described in a previous report (20). Endogenous peroxidase activity was blocked using 3% hydrogen peroxide, and the sections were incubated with diluted antibodies. A subsequent reaction was carried out with a biotin-free HRP enzyme–labeled polymer from the Envision Plus detection system (Dako Co.). Phospho-Smad2 antibody binding was detected using the Vectastain ABC Elite avidin/biotin/peroxidase kit (Vector Laboratories Inc.). A positive reaction was visualized with the addition of diaminobenzidine solution, which was followed by counterstaining with Mayer's hematoxylin. Primary antibodies for E-cadherin (1:100 dilution; BD), vimentin (1:50 dilution; Santa Cruz), CD44s (1:300 dilution; Bender MedSystems), and phospho-Smad2 (1:100 dilution; Cell Signaling) were used for this study. All of the immunohistochemical staining results were independently scored by 2 pathologists. The membranous E-cadherin, cytoplasmic vimentin, and membranous CD44s expressions were interpreted according to the guidelines published in previous studies (5, 25, 26). For membranous E-cadherin, cytoplasmic vimentin, membranous CD44s, and phospho-Smad2-positive nuclei, we graded the results into categories from 0 to 3+ as follows: 0, no staining; 1+, 1% to 25% staining; 2+, 26% to 50% staining; 3+, >50% of the specimen was stained. For membranous E-cadherin, the 2+ and 3+ samples were defined as positive immunohistochemical results. For cytoplasmic vimentin, membranous CD44s, and phospho-Smad2-positive nuclei, the 3+ specimens were defined as positive immunohistochemical results.

Statistical analyses

All of the experiments were carried out in triplicate, and the data shown are representative of the results. The data are presented as the means ± SD. Independent Student *t* tests were used to compare the continuous variables between the 2

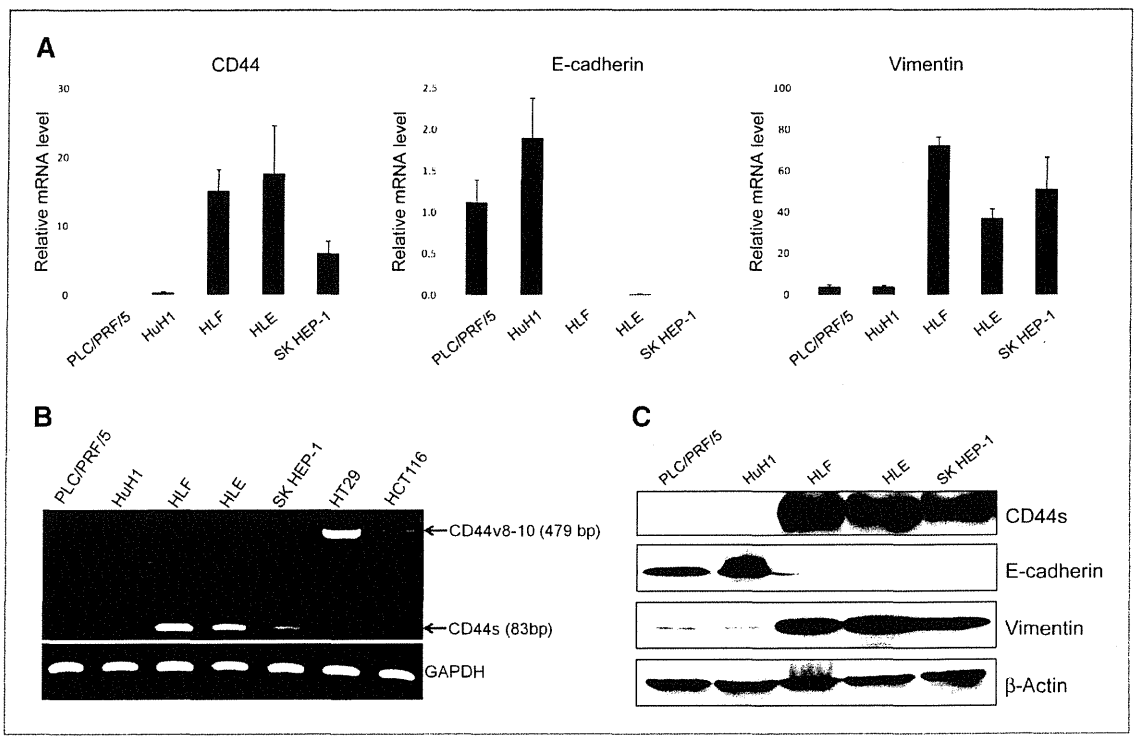

CD44s expression is associated with a mesenchymal phenotype in hepatocellular carcinoma cells. A, the relative expression levels of *CD44*, *E-cadherin*, and *vimentin* mRNA in 5 HCC cell lines are shown. The data represent the means ± SD ($n = 3$). B, RT-PCR analysis of CD44 mRNA in 5 HCC cell lines. Total RNA isolated from the 5 HCC cell lines was subjected to RT-PCR analysis with primers targeted to exons 5 and 16 of human CD44 cDNA and to human GAPDH cDNA. The positions of PCR products derived from CD44v8-10 (479 bp) or CD44s (83 bp) cDNAs are indicated. HT29 and HCT116 cell lines (colon cancer cell lines) were used as positive controls. C, the expression levels of CD44, E-cadherin, and vimentin protein in the 5 HCC cell lines, as determined by Western blot analysis.

Published OnlineFirst May 2, 2012; DOI:10.1158/0008-5472.CAN-12-0299

groups, and categorical variables were compared using the χ^2 test. Overall survival and disease-free survival were calculated using the Kaplan–Meier method and compared using the log-rank test. Statistical analyses were carried out as indicated with a statistical analysis software program (Excel Statistics, Social Survey Research Information Co.). Differences were considered to be significant if $P < 0.05$.

Results

CD44 standard isoform expression is associated with a mesenchymal phenotype in hepatocellular carcinoma cells

We examined the expression of CD44 and its association with EMT markers (E-cadherin and vimentin) in 5 HCC cell lines (PLC/PRF/5, HuH1, HLF, HLE, and SK HEP-1). At the mRNA level, the high CD44 expressing cell lines HLF, HLE, and SK HEP-1 showed high expression levels of vimentin, whereas the low CD44 expressing cell lines PLC/PRF/5 and HuH1 showed high expression levels of E-cadherin, as determined by real-time PCR (Fig. 1A). Recently, we showed that the CD44 isoform expressed in the tumor cells of Gan mice, as well as in human gastrointestinal cell lines, consists mostly of variant isoforms (CD44v8-10) containing amino acids derived from exons 8 to 10 (18, 27). To determine the predominant isoform of CD44 expressed in the HCC cell lines, we examined the expression levels of the different isoforms using RT-PCR according to the same method. Unlike in human colon cancer cell lines, our RT-PCR analysis revealed that CD44s mRNA, rather than CD44v8-10mRNA, was the dominant form present in the human HCC cell lines HLF, HLE, and SK HEP-1 (Fig. 1B). We confirmed the associations of CD44s with E-cadherin and vimentin expression at the protein level (Fig. 1C). These results suggested that high levels of CD44s expression are related to a mesenchymal phenotype, which includes downregulation of E-cadherin and upregulation of vimentin, in HCC cells. We also examined the expression of other CSC markers that were previously reported in HCC (12, 28–31) and compared them with the expression of E-cadherin and vimentin. However, no correlations were observed that were similar to that of CD44 and vimentin. In addition, the expression levels of EpCAM, CD133, and CD13 seemed to be similar to the expression level of E-cadherin (Supplementary Fig. S1).

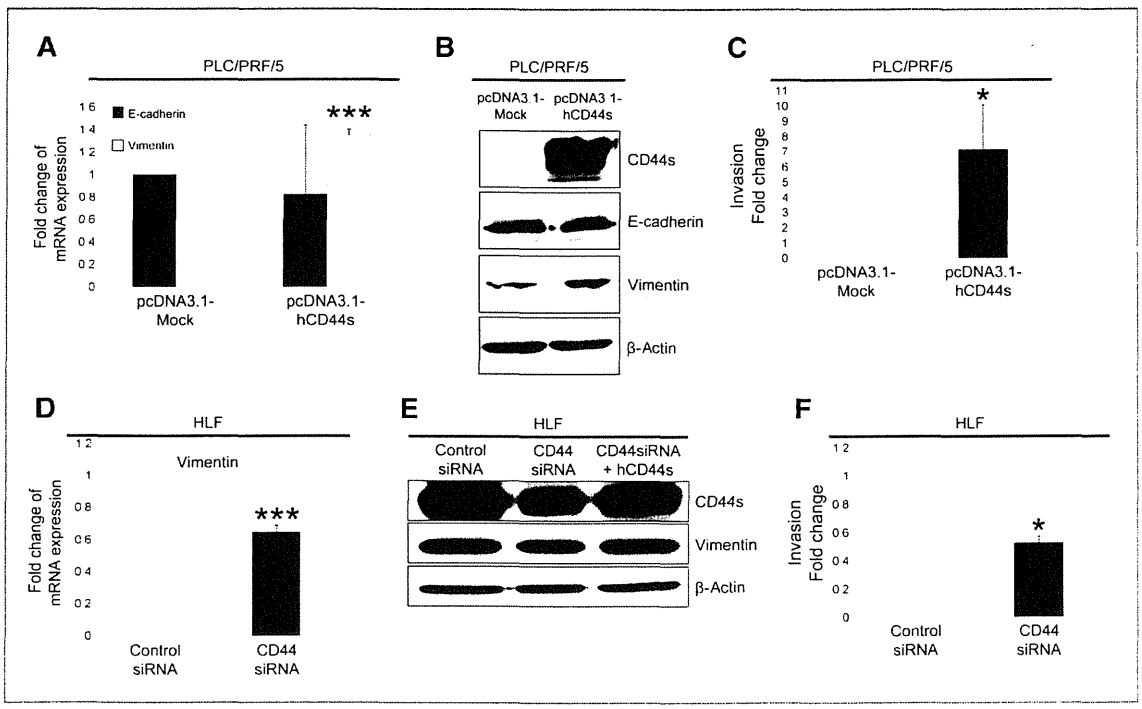

Figure 2. Overexpression of CD44s promotes the expression of vimentin and tumor invasiveness of hepatocellular carcinoma cells whereas the knockdown of CD44s attenuates these changes. A, the relative expression levels of *E-cadherin* and *vimentin* mRNA in PLC/PRF/5 cells overexpressing *CD44s* compared with control cells. The data represent the means ± SD ($n = 3$; ***, $P < 0.001$). B, the expression levels of CD44s, E-cadherin, and vimentin proteins in PLC/PRF/5 cells overexpressing CD44s compared with control cells. C, the invasive capacity of PLC/PRF/5 cells overexpressing CD44s compared with control cells. The data represent the means ± SD ($n = 3$; *, $P < 0.05$). D, the relative expression levels of *vimentin* mRNA in HLF cells transfected with siRNA targeted against CD44 compared with control cells. The data represent the means ± SD ($n = 3$; ***, $P < 0.001$). E, the expression levels of CD44s and vimentin protein in HLF cells transfected with siRNA targeted against CD44 or transfected with both siRNA targeted against CD44 and an hCD44s expression vector compared with control cells. F, the invasive capacity of HLF cells transfected with siRNA targeted against CD44 compared with control cells. The data represent the means ± SD ($n = 3$; *, $P < 0.05$).

Published OnlineFirst May 2, 2012; DOI:10.1158/0008-5472.CAN-12-0299

Overexpression of CD44s promotes the expression of vimentin and tumor invasiveness of hepatocellular carcinoma cells, whereas the knockdown of CD44s attenuates these changes

To investigate whether CD44s regulates the mesenchymal phenotype of HCC cells, we transiently transfected PLC/PRF/5 cells with a human CD44s expression vector. The overexpression of CD44s increased the expression of vimentin but did not decrease the expression of E-cadherin (Fig. 2A and B). Furthermore, the overexpression of CD44s increased the *in vitro* invasion of the transfected cells by 7-fold (Fig. 2C). Next, we examined the effect of the siRNA knockdown of CD44 in HLF cells, which normally have high CD44 expression, to determine whether CD44s is essential for the expression of vimentin in HCC cells. CD44 siRNA attenuated the expression of vimentin at the mRNA and protein levels (Fig. 2D and E). Furthermore, in HLF cells pretreated with CD44 siRNA, the addition of a CD44s expression vector reversibly increased the expression of vimentin (Fig. 2E). The results from an *in vitro* invasion assay revealed that HLF cells transfected with CD44 siRNA exhibited a decrease in invasion compared with cells transfected with a control siRNA (Fig. 2F). We observed similar results in high CD44s expressing HLE and SK HEP-1 cells (Supplementary Fig. S2). Overexpression of CD44s in PLC/PRF/5 cells did not decrease the expression of E-cadherin. Moreover, we could not detect the upregulation of E-cadherin in the CD44 knockdown cells. These results suggested that CD44s regulates the expression of vimentin and tumor cell invasion in HCC cells.

CD44s is induced by TGF-β and regulates the TGF-β–mediated mesenchymal phenotype in hepatocellular carcinoma cells

TGF-β signaling is central to tumorigenesis and tumor progression because it regulates many critical cellular processes, including cell proliferation, EMT, and stem cell maintenance (32). HLF and HLE cells express detectable levels of phosphorylated Smad2, and the expression of E-cadherin was increased after incubation with a TGFβ type I receptor kinase inhibitor in HLF and HLE cells, suggesting that TGF-β signaling plays a crucial role in EMT in HCC cells (33). TGF-β1 is overexpressed in tumor cells, and this overexpression correlates with a poor prognosis in patients with HCC (34, 35). Thus, we investigated the role of CD44 in TGF-β signaling. We screened the activation status of TGF-β signaling by measuring phosphorylated Smad2 (phospho-Smad2) expression in the 5 HCC cell lines. As reported previously, HLF and HLE cells expressed detectable levels of phosphorylated Smad2 whereas SK HEP-1 cells did not (Fig. 3A). The precise mechanism of CD44 expression in SK HEP-1 cells with low phospho-Smad2 expression is unclear from our study. SK HEP-1 cells are originally derived from endothelial cells, which express CD44

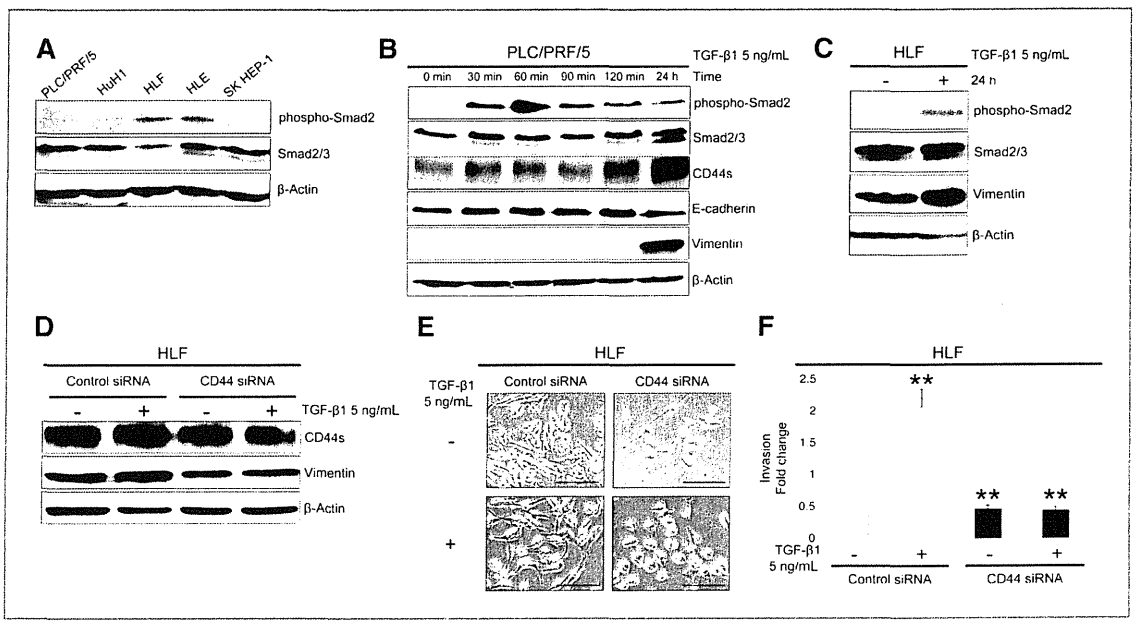

CD44s is induced by TGF-β1 and regulates the TGF-β–mediated mesenchymal phenotype in hepatocellular carcinoma cells. A, the expression of phosphorylated Smad2 (phospho-Smad2) in the 5 HCC cell lines, as determined by Western blot analysis. B, immunoblot analysis of phospho-Smad2 and the expression levels of CD44s, E-cadherin, and vimentin following TGF-β1 (5 ng/mL) treatment in PLC/PRF/5 cells. C, immunoblot analysis of phospho-Smad2 and the expression level of vimentin following TGF-β1 (5 ng/mL) treatment in HLF cells. D, immunoblot analysis of the expression levels of CD44s and vimentin with or without TGF-β1 (5 ng/mL) treatment for 24 hours in HLF cells transfected with siRNA targeted against CD44 compared with control cells. E, phase-contrast images with or without TGF-β1 (5 ng/mL) treatment for 24 hours in the HLF cells transfected with siRNA targeted against CD44 compared with control cells. Scale bars, 200 μm. F, the invasive capacity of HLF cells with or without TGF-β1 (5 ng/mL) treatment for 24 hours after transfection with siRNA targeted against CD44 compared with untreated control cells. The data represent the means ± SD ($n = 3$; **, $P < 0.01$).

Published OnlineFirst May 2, 2012; DOI:10.1158/0008-5472.CAN-12-0299

(36, 37). In human endothelial cells, other growth factors, such as basic fibroblast growth factor, VEGF, and hepatocyte growth factor/scatter factor (HGF/SF), can induce the expression of CD44 (37, 38). Therefore, an alternative mechanism may be associated with the expression of CD44 in SK HEP-1 cells. We next examined the role of CD44 in the TGF-β–mediated mesenchymal phenotype of HCC cells. Treatment with TGF-β1 induced a mesenchymal spindle-like morphology in PLC/PRF/5 cells (Supplementary Fig. S3A). Following treatment with TGF-β1 (5 ng/mL), phospho-Smad2 expression in PLC/PRF/5 cells progressively increased in a time-dependent manner and peaked after 60 minutes (Fig. 3B). The downregulation of E-cadherin, the upregulation of vimentin, and the expression of CD44s were induced after 24 hours of treatment with TGF-β1 in PLC/PRF/5 cells (Fig. 3B). The expression of E-cadherin mRNA was decreased after 6 hours and restored after 24 hours (Supplementary Fig. S3B). The expression of vimentin and CD44 mRNA were elevated after 24 hours. Several transcription factors, including Snail, Slug, and Twist1 promote EMT in epithelial cells (4). The expression of Snail mRNA was increased after treatment with TGF-β1 and peaked after 3 hours (Supplementary Fig. S3C). The expression of Slug was not affected, and no expression of Twist1 in response to TGF-β1 was detected in PLC/PRF/5 cells. These results suggested that TGF-β signaling triggered the mesenchymal phenotype and induced the expression of CD44s in HCC cells. Next, we examined the effects of CD44s on the TGF-β–mediated mesenchymal phenotype. HLF cells also displayed progressively increased phospho-Smad2 levels in a time-dependent manner following incubation with TGF-β1 (5 ng/mL), and the levels peaked after 60 minutes (Supplementary Fig. S3D). In addition, upregulation of vimentin was induced by TGF-β1 after 24 hours

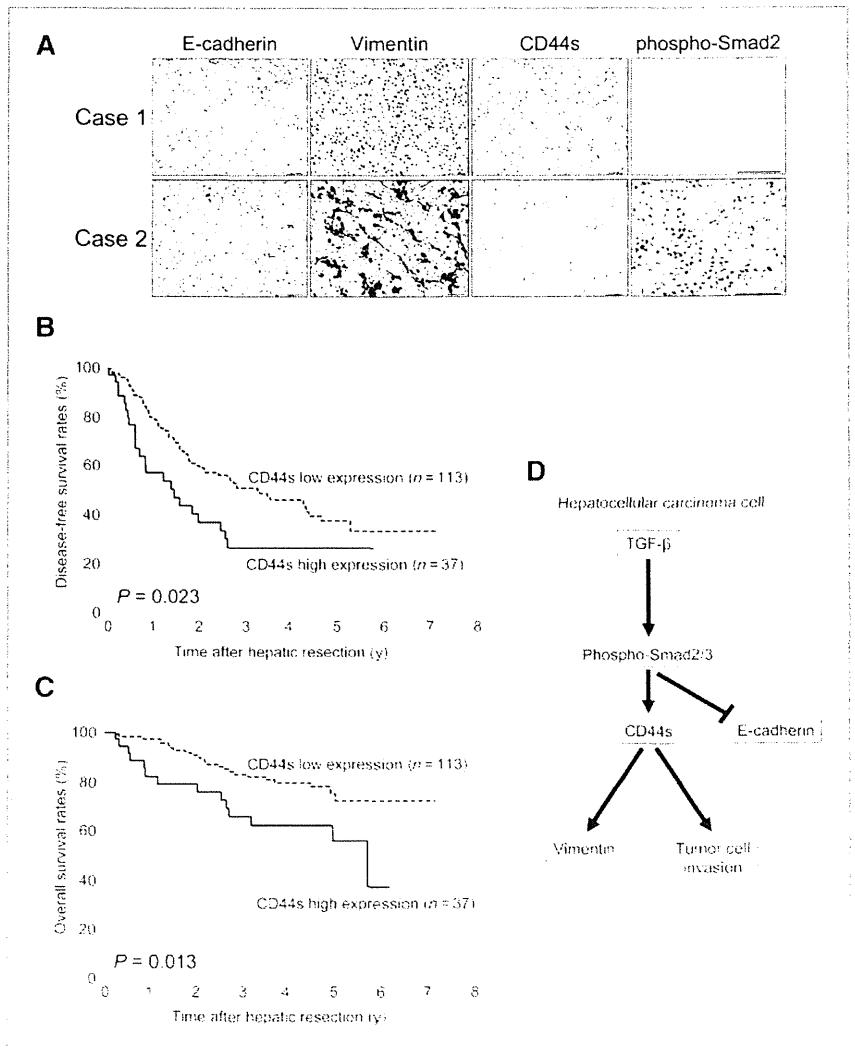

Figure 4. CD44s expression is associated with E-cadherin and vimentin expression and poor prognosis in patients with hepatocellular carcinoma. A, immunohistochemical staining of E-cadherin, vimentin, CD44s, and phospho-Smad2 in representative cases with low CD44s expression (case 1) and high CD44s expression (case 2). Scale bars, 50 μm. B, Kaplan–Meier survival analysis of disease-free survival in 150 HCC patients comparing the high CD44s expression group and the low CD44s expression group using the log-rank test. C, Kaplan–Meier survival analysis of overall survival in 150 HCC patients comparing the high CD44s expression group and the low CD44s expression group using the log-rank test. D, model of the regulation of the mesenchymal phenotype by CD44s in hepatocellular carcinoma cells following the induction of CD44s expression by TGF-β signaling. Subsequently, CD44s promotes vimentin expression and tumor cell invasion. The expression of E-cadherin may be suppressed by other mechanisms in the TGF-β signaling pathway.

Published OnlineFirst May 2, 2012; DOI:10.1158/0008-5472.CAN-12-0299

Table 1. [illegible]

	E-cadherin			Vimentin			phospho-Smad2 nuclear positivity		
	Low (n = 92)	High (n = 58)	P^a	Low (n = 126)	High (n = 24)	P^a	Low (n = 123)	High (n = 27)	P^a
CD44s									
Low (n = 113)	64	49	0.039	108	5	<0.001	106	7	<0.001
High (n = 37)	28	9		18	19		17	20	

Abbreviations: CD44s, CD44 standard isoform; phospho-Smad2, phosphorylated Smad2.
[a]Estimated by χ^2 test.

of treatment in HLF cells (Fig. 3C). These results indicated that TGF-β signaling enhances the expression of vimentin in HLF cells. CD44 siRNA inhibited the TGF-β–mediated vimentin expression, mesenchymal spindle-like morphology, and tumor invasiveness in HLF cells (Fig. 3D–F). These results suggested that CD44s is essential for the TGF-β–mediated mesenchymal phenotype in HCC cells.

CD44s expression is associated with E-cadherin and vimentin expression and poor prognosis in patients with hepatocellular carcinoma

To confirm the *in vitro* finding that the TGF-β–mediated mesenchymal phenotype and induction of CD44s are correlated in HCC cells, we analyzed the expression levels of CD44s, E-cadherin, vimentin, and phospho-Smad2 by IHC in 150 HCC patient samples. High expression of CD44s (e.g., case 2 shown in Fig. 4A) was detected in 25% (37 of 150) of the samples, and low E-cadherin expression was significantly associated with high vimentin expression (P = 0.004). High CD44s expression was significantly associated with low E-cadherin expression (P = 0.039), high vimentin expression (P < 0.001), and high phospho-Smad2 nuclear positivity (P < 0.001; Table 1). These data suggested that the activation of TGF-β signaling induces CD44s expression and a mesenchymal phenotype in patients with HCC. With regard to clinicopathologic factors, a significant correlation was shown between high CD44s expression and large tumor size (P = 0.003), multiple tumors (P = 0.032), and poor tumor differentiation (P = 0.020; Table 2). We further investigated the association between the expression levels of CD44s, vimentin, and E-cadherin and the clinicopathologic factors in HCC patients. In a subgroup of patients with a CD44s^{high}/vimentin^{high}/E-cadherin^{low} expression profile, the

Table 2. Correlation between CD44s expression and the clinicopathologic factors of 150 HCC patients

	CD44s high expression (n = 37)	CD44s low expression (n = 113)	P
Age: ≤60/>60 (y)	9/28	35/78	0.441
Sex: Male/Female	30/7	93/20	0.867
HBs-Ag: Negative/Positive	28/9	79/34	0.501
HCV-Ab: Negative/Positive	20/17	61/52	0.994
Child–Pugh classification: A/B	32/5	103/10	0.412
AFP: ≤20/>20 (ng/mL)	16/21	60/53	0.298
PIVKA-II: ≤107/>107 (mAU/mL)	18/19	57/56	0.850
Tumor size: ≤3/>3 (cm)	5/32	45/68	**0.003**
Tumor number: 1/2≤	21/16	85/28	**0.032**
Tumor encapsulation: Absent/present	2/35	15/98	0.190
Tumor differentiation: Moderate, well/poor	25/12	96/17	**0.020**
LCSGJ TNM Stage: 1,2/3, 4	18/19	71/42	0.127
AJCC/UICC TNM Stage: 1,2/3, 4	28/9	94/19	0.309
Vascular invasion: Absent/present	30/7	102/11	0.136

NOTE: Vascular invasion, portal vein (3rd branch, 2nd branch, 1st branch, or trunk) or hepatic vein (trunk of hepatic vein or IVC) invasion were defined via macroscopic examination of the resected specimens.
Abbreviations: CD44s, CD44 standard isoform; HBs-Ag, hepatitis B surface antigen; HCV-Ab, hepatitis C antibody; AFP, α-fetoprotein; PIVKA II, protein-induced vitamin K absence-II; LCSGJ, Liver Cancer Study Group of Japan.

Published OnlineFirst May 2, 2012; DOI:10.1158/0008-5472.CAN-12-0299

incidence of vascular invasion was significantly higher than that in a subgroup of patients with a CD44s^{low}/vimentin^{low}/E-cadherin^{high} expression profile (25% vs. 0%, respectively, $P < 0.001$; Supplementary Table S1). In all 150 HCC patients studied, high CD44s expression was more associated with frequent vascular invasion than low CD44s expression was, but this correlation did not reach a statistically significant difference (19% vs. 10%, $P = 0.136$). These results suggested that not only the mesenchymal phenotype via CD44s but also the loss of E-cadherin expression plays an important role of the vascular invasion in HCC patients. Notably, high CD44s expression was significantly associated with shorter disease-free survival ($P = 0.023$; Fig. 4B) and shorter overall survival ($P = 0.013$; Fig. 4C).

Discussion

In this study, CD44s, but not the variant isoforms, regulates the mesenchymal phenotype in HCC cells. In patients with HCC, tumoral CD44s overexpression was associated with the mesenchymal phenotype, as characterized by low E-cadherin expression and high vimentin expression. Interestingly, CD44s mRNA was the dominant form of CD44 mRNA present in human HCC cell lines, whereas the presence of high levels of the CD44v have been proposed as an important metastatic tumor marker in a number of cancers such as colon and lung cancer (39, 40). In breast cancer, CD44s was essential for the response to TGF-β during EMT, and the gain of CD44s expression was accompanied by a loss of expression of the variant isoforms (41). These findings suggest that the dominant form of CD44 isoforms in different tumors varies according to the location of the cancer cells.

TGF-β primes cancer cells for pulmonary metastasis and metastatic colonization of cancer cells in bones (42, 43). A recent study showed that TGF-β in the blood activates TGF-β signaling in cancer cells, resulting in their transition to an invasive mesenchymal-like phenotype with enhanced metastatic potential (44). Furthermore, a link between TGF-β and the CD44^{high} population has been described in breast cancer and glioblastoma. TGF-β increases the CD44^{high}/CD24^{low} population, which is enriched in CSCs, through the induction of EMT in breast cancer (8). In addition, glioma-initiating cells (GIC) expressed high levels of CD44, and the inhibition of TGF-β signaling decreased the GIC population in glioblastomas (45). These results agree with our studies showing a novel role for CD44s in the TGF-β–mediated mesenchymal phenotype in HCC cells.

Although TGF-β signaling can induce the mesenchymal phenotype as characterized by low E-cadherin expression and high vimentin expression in epithelial cells, the mediators between TGF-β signaling and the mesenchymal phenotype are still unclear. This study suggests that CD44 plays a downstream role in TGF-β signaling by regulating the expression of vimentin and tumor cell invasiveness, and that CD44 does not affect the expression of E-cadherin, which may be suppressed by other mechanisms involved in the TGF-β pathway (Fig. 4D). The expression of Snail was elevated after 3 hours, and the expression of E-cadherin was suppressed after 6 hours. The induction of Snail expression in response to TGF-β is mediated by Smad2/3. Smad3 binds to the *Snail* promoter and activates its transcription (46). Smad3/4 and Snail interact to form a transcriptional repressor complex, which targets the promoter of E-cadherin (47). The time course of the activation of TGF-β signaling and the expression of Snail and E-cadherin in this study suggested that TGF-β signaling may suppress the expression of E-cadherin via Snail in HCC cells.

We showed that high CD44s expression was a poor prognostic factor following curative hepatic resection of primary HCC. In addition to CD44s, several other variant isoforms (CD44v5, CD44v6, CD44v7-8, and CD44v10) correlate with a worse prognosis in HCC patients, as determined by immunohistochemical analysis (26). Our investigations about clinicopathologic factors showed a significant correlation between CD44s expression and large tumor size, multiple tumors, and poor tumor differentiation in patients with HCC. Consistent with our *in vitro* analysis, high CD44s expression correlated with high vimentin expression in human HCC cells. Furthermore, in patients with HCC, we showed that phospho-Smad2 nuclear positivity was associated with high CD44s expression and that a CD44s^{high}/vimentin^{high}/E-cadherin^{low} expression profile was associated with vascular invasion. Together with our *in vitro* studies, these results suggested that the TGF-β–CD44s axis plays an important role in the vascular invasion of HCC. TGF-β signaling was recently determined to maintain the stem cell–like properties of tumor-initiating cells (32). Chaffer and Weinberg suggested a new concept of cancer cell metastasis in which cancer cells traveling through the circulation system are considered to be CSCs because of their anchorage-independent survival and the fact that these CSCs extravasate and invade into the parenchyma at distant organs (48). These observations support our findings that CD44s, a CSC marker, plays a downstream role in TGF-β signaling in HCC cells. We are continuing our studies to examine whether CD44s has an important role in the modulation of CSC properties in HCC cells.

In conclusion, our study suggests that the standard isoform of CD44, a CSC marker, regulates the TGF-β–mediated mesenchymal phenotype, and that its expression indicates poor prognosis in patients with HCC. This information will be valuable for a better understanding of the relationship between CSCs and the mesenchymal phenotype induced by EMT; in addition, our results establish CD44s as a novel therapeutic target for HCC.

Disclosure of Potential Conflicts of Interest

No potential conflicts of interest were disclosed.

Authors' Contributions

Conception and design: K. Mima, H. Okabe, T. Ishimoto
Development of methodology: K. Mima, H. Okabe, H. Baba
Acquisition of data (provided animals, acquired and managed patients, provided facilities, etc.): H. Okabe, S. Nakagawa, H. Kuroki, O. Nagano, H. Baba
Analysis and interpretation of data (e.g., statistical analysis, biostatistics, computational analysis): K. Mima, H. Okabe, H. Hayashi, H. Kuroki, M. Watanabe, H. Baba
Writing, review, and/or revision of the manuscript: K. Mima, H. Okabe, H. Hayashi, T. Beppu, H. Baba

Published OnlineFirst May 2, 2012; DOI:10.1158/0008-5472.CAN-12-0299

Administrative, technical, or material support (i.e., reporting or organizing data, constructing databases): H. Okabe, S. Nakagawa, M. Tamada
Study supervision: K. Mima, H. Okabe, M. Watanabe, H. Saya

Acknowledgments

The authors thank Keisuke Miyake and Naoko Yokoyama for their valuable technical assistance and also Eri Takahashi for her useful suggestions.

The costs of publication of this article were defrayed in part by the payment of page charges. This article must therefore be hereby marked *advertisement* in accordance with 18 U.S.C. Section 1734 solely to indicate this fact.

Received January 30, 2012; revised April 7, 2012; accepted April 25, 2012; published OnlineFirst May 2, 2012.

References

1. El-Serag HB. Hepatocellular carcinoma. N Engl J Med 2011;365:1118–27.
2. Poon RT, Ng IO, Fan ST, Lai EC, Lo CM, Liu CL, et al. Clinicopathologic features of long-term survivors and disease-free survivors after resection of hepatocellular carcinoma: a study of a prospective cohort. J Clin Oncol 2001;19:3037–44.
3. Polyak K, Weinberg RA. Transitions between epithelial and mesenchymal states: acquisition of malignant and stem cell traits. Nat Rev Cancer 2009;9:265–73.
4. Thiery JP, Acloque H, Huang RY, Nieto MA. Epithelial-mesenchymal transitions in development and disease. Cell 2009;139:871–90.
5. Yang MH, Chen CL, Chau GY, Chiou SH, Su CW, Chou TY, et al. Comprehensive analysis of the independent effect of twist and snail in promoting metastasis of hepatocellular carcinoma. Hepatology 2009;50:1464–74.
6. Lee TK, Poon RT, Yuen AP, Ling MT, Kwok WK, Wang XH, et al. Twist overexpression correlates with hepatocellular carcinoma metastasis through induction of epithelial-mesenchymal transition. Clin Cancer Res 2006;12:5369–76.
7. Chen L, Chan TH, Yuan YF, Hu L, Huang J, Ma S, et al. CHD1L promotes hepatocellular carcinoma progression and metastasis in mice and is associated with these processes in human patients. J Clin Invest 2010;120:1178–91.
8. Mani SA, Guo W, Liao MJ, Eaton EN, Ayyanan A, Zhou AY, et al. The epithelial-mesenchymal transition generates cells with properties of stem cells. Cell 2008;133:704–15.
9. Ponta H, Sherman L, Herrlich PA. CD44: from adhesion molecules to signalling regulators. Nat Rev Mol Cell Biol 2003;4:33–45.
10. Zoller M. CD44: can a cancer-initiating cell profit from an abundantly expressed molecule? Nat Rev Cancer 2011;11:254–67.
11. Clevers H. The cancer stem cell: premises, promises and challenges. Nat Med 2011;17:313–9.
12. Yang ZF, Ho DW, Ng MN, Lau CK, Yu WC, Ngai P, et al. Significance of CD90 + cancer stem cells in human liver cancer. Cancer Cell 2008;13:153–66.
13. Al-Hajj M, Wicha MS, Benito-Hernandez A, Morrison SJ, Clarke MF. Prospective identification of tumorigenic breast cancer cells. Proc Natl Acad Sci U S A 2003;100:3983–8.
14. Dalerba P, Dylla SJ, Park IK, Liu R, Wang X, Cho RW, et al. Phenotypic characterization of human colorectal cancer stem cells. Proc Natl Acad Sci U S A 2007;104:10158–63.
15. Prince ME, Sivanandan R, Kaczorowski A, Wolf GT, Kaplan MJ, Dalerba P, et al. Identification of a subpopulation of cells with cancer stem cell properties in head and neck squamous cell carcinoma. Proc Natl Acad Sci U S A 2007;104:973–8.
16. Li C, Heidt DG, Dalerba P, Burant CF, Zhang L, Adsay V, et al. Identification of pancreatic cancer stem cells. Cancer Res 2007;67:1030–7.
17. Scheel C, Eaton EN, Li SH, Chaffer CL, Reinhardt F, Kah KJ, et al. Paracrine and autocrine signals induce and maintain mesenchymal and stem cell states in the breast. Cell 2011;145:926–40.
18. Ishimoto T, Nagano O, Yae T, Tamada M, Motohara T, Oshima H, et al. CD44 variant regulates redox status in cancer cells by stabilizing the xCT subunit of system xc(-) and thereby promotes tumor growth. Cancer Cell 2011;19:387–400.
19. Hiyoshi Y, Kamohara H, Karashima R, Sato N, Imamura Y, Nagai Y, et al. MicroRNA-21 regulates the proliferation and invasion in esophageal squamous cell carcinoma. Clin Cancer Res 2009;15:1915–22.
20. Okabe H, Beppu T, Hayashi H, Ishiko T, Masuda T, Otao R, et al. Hepatic stellate cells accelerate the malignant behavior of cholangiocarcinoma cells. Ann Surg Oncol 2011;18:1175–84.
21. Livak KJ, Schmittgen TD. Analysis of relative gene expression data using real-time quantitative PCR and the 2(-Delta Delta C(T)) Method. Methods 2001;25:402–8.
22. Japan LCSGJ. The general rules for the clinical and pathological study of primary liver cancer. 5th ed., revised version. Tokyo: Kanehara; 2009.
23. Minagawa M, Ikai I, Matsuyama Y, Yamaoka Y, Makuuchi M. Staging of hepatocellular carcinoma: assessment of the Japanese TNM and AJCC/UICC TNM systems in a cohort of 13,772 patients in Japan. Ann Surg 2007;245:909–22.
24. Vauthey JN, Lauwers GY, Esnaola NF, Do KA, Belghiti J, Mirza N, et al. Simplified staging for hepatocellular carcinoma. J Clin Oncol 2002;20:1527–36.
25. Yang MH, Hsu DS, Wang HW, Wang HJ, Lan HY, Yang WH, et al. Bmi1 is essential in Twist1-induced epithelial-mesenchymal transition. Nat Cell Biol 2010;12:982–92.
26. Endo K, Terada T. Protein expression of CD44 (standard and variant isoforms) in hepatocellular carcinoma: relationships with tumor grade, clinicopathologic parameters, p53 expression, and patient survival. J Hepatol 2000;32:78–84.
27. Ishimoto T, Oshima H, Oshima M, Kai K, Torii R, Masuko T, et al. CD44 + slow-cycling tumor cell expansion is triggered by cooperative actions of Wnt and prostaglandin E2 in gastric tumorigenesis. Cancer Sci 2010;101:673–8.
28. Chiba T, Miyagi S, Saraya A, Aoki R, Seki A, Morita Y, et al. The polycomb gene product BMI1 contributes to the maintenance of tumor-initiating side population cells in hepatocellular carcinoma. Cancer Res 2008;68:7742–9.
29. Yamashita T, Ji J, Budhu A, Forgues M, Yang W, Wang HY, et al. EpCAM-positive hepatocellular carcinoma cells are tumor-initiating cells with stem/progenitor cell features. Gastroenterology 2009;136:1012–24.
30. Ma S, Chan KW, Hu L, Lee TK, Wo JY, Ng IO, et al. Identification and characterization of tumorigenic liver cancer stem/progenitor cells. Gastroenterology 2007;132:2542–56.
31. Haraguchi N, Ishii H, Mimori K, Tanaka F, Ohkuma M, Kim HM, et al. CD13 is a therapeutic target in human liver cancer stem cells. J Clin Invest 2010;120:3326–39.
32. Ikushima H, Miyazono K. TGFbeta signalling: a complex web in cancer progression. Nat Rev Cancer 2010;10:415–24.
33. Fransvea E, Angelotti U, Antonaci S, Giannelli G. Blocking transforming growth factor-beta up-regulates E-cadherin and reduces migration and invasion of hepatocellular carcinoma cells. Hepatology 2008;47:1557–66.
34. Bedossa P, Peltier E, Terris B, Franco D, Poynard T. Transforming growth factor-beta 1 (TGF-beta 1) and TGF-beta 1 receptors in normal, cirrhotic, and neoplastic human livers. Hepatology 1995;21:760–6.
35. Abou-Shady M, Baer HU, Friess H, Berberat P, Zimmermann A, Graber H, et al. Transforming growth factor betas and their signaling receptors in human hepatocellular carcinoma. Am J Surg 1999;177:209–15.
36. Heffelfinger SC, Hawkins HH, Barrish J, Taylor L, Darlington GJ. SK HEP-1: a human cell line of endothelial origin. In Vitro Cell Dev Biol 1992;28A:136–42.
37. Griffioen AW, Coenen MJ, Damen CA, Hellwig SM, van Weering DH, Vooys W, et al. CD44 is involved in tumor angiogenesis; an activation antigen on human endothelial cells. Blood 1997;90:1150–9.
38. Hiscox S, Jiang WG. Regulation of endothelial CD44 expression and endothelium-tumour cell interactions by hepatocyte growth factor/scatter factor. Biochem Biophys Res Commun 1997;233:1–5.

Published OnlineFirst May 2, 2012; DOI:10.1158/0008-5472.CAN-12-0299

39. Kuniyasu H, Oue N, Tsutsumi M, Tahara E, Yasui W. Heparan sulfate enhances invasion by human colon carcinoma cell lines through expression of CD44 variant exon 3. Clin Cancer Res 2001;7:4067–72.
40. Miyoshi T, Kondo K, Hino N, Uyama T, Monden Y. The expression of the CD44 variant exon 6 is associated with lymph node metastasis in non-small cell lung cancer. Clin Cancer Res 1997;3:1289–97.
41. Brown RL, Reinke LM, Damerow MS, Perez D, Chodosh LA, Yang J, et al. CD44 splice isoform switching in human and mouse epithelium is essential for epithelial-mesenchymal transition and breast cancer progression. J Clin Invest 2011;121:1064–74.
42. Padua D, Zhang XH, Wang Q, Nadal C, Gerald WL, Gomis RR, et al. TGFbeta primes breast tumors for lung metastasis seeding through angiopoietin-like 4. Cell 2008;133:66–77.
43. Yin JJ, Selander K, Chirgwin JM, Dallas M, Grubbs BG, Wieser R, et al. TGF-beta signaling blockade inhibits PTHrP secretion by breast cancer cells and bone metastases development. J Clin Invest 1999;103:197–206.
44. Labelle M, Begum S, Hynes RO. Direct signaling between platelets and cancer cells induces an epithelial-mesenchymal-like transition and promotes metastasis. Cancer Cell 2011;20:576–90.
45. Anido J, Saez-Borderias A, Gonzalez-Junca A, Rodon L, Folch G, Carmona MA, et al. TGF-beta receptor inhibitors target the CD44(high)/Id1(high) glioma-initiating cell population in human glioblastoma. Cancer Cell 2010;18:655–68.
46. Hoot KE, Lighthall J, Han G, Lu SL, Li A, Ju W, et al. Keratinocyte-specific Smad2 ablation results in increased epithelial-mesenchymal transition during skin cancer formation and progression. J Clin Invest 2008;118:2722–32.
47. Vincent T, Neve EP, Johnson JR, Kukalev A, Rojo F, Albanell J, et al. A SNAIL1-SMAD3/4 transcriptional repressor complex promotes TGF-beta mediated epithelial-mesenchymal transition. Nat Cell Biol 2009;11:943–50.
48. Chaffer CL, Weinberg RA. A perspective on cancer cell metastasis. Science 2011;331:1559–64.

Original article

External biliary drainage and liver regeneration after major hepatectomy

R. Otao[1], T. Beppu[1,2], T. Isiko[1], K. Mima[1], H. Okabe[1], H. Hayashi[1], T. Masuda[1], A. Chikamoto[1], H. Takamori[1] and H. Baba[1]

[1]Department of Gastroenterological Surgery, Graduate School of Medical Sciences, Kumamoto University, and [2]Department of Multidisciplinary Treatment for Gastroenterological Cancer, Innovation Centre for Translational Research, Kumamoto University Hospital, Kumamoto, Japan
Correspondence to: Professor H. Baba, Department of Gastroenterological Surgery, Graduate School of Medical Sciences, Kumamoto University, 1-1-1 Honjo, Kumamoto 860-8556, Japan (e-mail: hdobaba@kumamoto-u.ac.jp)

Background: Bile acid signalling and farnesoid X receptor activation are assumed to be essential for liver regeneration. This study was designed to investigate the association between serum bile acid levels and extent of liver regeneration after major hepatectomy.

Methods: Patients who underwent left- or right-sided hemihepatectomy between 2006 and 2009 at the authors' institution were eligible for inclusion. Patients were divided into two groups: those undergoing hemihepatectomy with external bile drainage by cystic duct tube (group 1) and those having hemihepatectomy without drainage (group 2). Serum bile acid levels were measured before and after hepatectomy. Computed tomography was used to calculate liver volume before hepatectomy and remnant liver volume on day 7 after surgery.

Results: A total of 46 patients were enrolled. Mean(s.d.) serum bile acid levels on day 3 after hemihepatectomy were significantly higher in group 2 than in group 1 (11·6(13·5) *versus* 2·7(2·1) μmol/l; $P = 0·003$). Regenerated liver volumes on day 7 after hepatectomy were significantly greater in group 2 138·1(135·9) ml *versus* 40·0(158·8) ml in group 1; $P = 0·038$). Liver regeneration volumes and rates on day 7 after hemihepatectomy were positively associated with serum bile acid levels on day 3 after hemihepatectomy ($P = 0·006$ and $P < 0·001$ respectively). The incidence of bile leakage was similar in the two groups.

Conclusion: Initial liver regeneration after major hepatectomy was less after biliary drainage and was associated with serum bile acid levels. External biliary drainage should be used judiciously after liver resection.

Paper accepted 29 June 2012
Published online in Wiley Online Library (www.bjs.co.uk). **DOI:** 10.1002/bjs.8906

Introduction

Hepatic resection is one of the most effective treatments for patients with liver tumours[1]. However, major hepatectomy is associated with high rates of morbidity and mortality because of deterioration of liver function. In Japan, most patients with hepatocellular carcinoma have relatively poor hepatic functional reserve owing to chronic liver disorders such as hepatitis B or C infection[2]. In this context, sufficient liver regeneration after major hepatectomy is important to prevent postoperative liver failure.

Previous experimental animal studies have revealed that bile acid signalling and farnesoid X receptor (FXR) activation are essential for early liver regeneration[3–5]. FXR belongs to the nuclear receptor superfamily and is highly expressed in liver and intestine. Increased serum bile acid levels accelerate, whereas decreased levels inhibit, liver regeneration after partial hepatectomy[3]. Preoperative external biliary drainage compared with internal biliary drainage leads to loss of bile acid and results in delayed liver regeneration after partial hepatectomy in rats[6–8].

Bile acid signalling has previously been demonstrated to be essential for liver regeneration after portal vein embolization (PVE) in humans[9]. However, limited data are available regarding the involvement of bile acid signalling in liver regeneration after partial hepatectomy in humans. This study investigated the association between external

biliary drainage and extent of liver regeneration after major hepatectomy in humans.

Methods

All patients undergoing right or left hepatectomy between July 2006 and December 2009 at the Department of Gastroenterological Surgery, Graduate School of Medical Sciences, Kumamoto University, were eligible for inclusion in the study, which was conducted as a retrospective analysis of a prospectively collected database. Only patients who underwent (extended) hemihepatectomy were selected to avoid the effects of small or complex resections on liver regeneration. Patients with previous PVE, other combined operative procedures, macroscopic portal vein tumour thrombus, or insufficient perioperative data or diagnostic images were excluded. Selected patients were classified into two groups according to the surgical procedure performed. Group 1 consisted of patients who underwent hemihepatectomy with external bile drainage by a cystic duct tube (C tube) to reduce the rate of postoperative biliary leakage[10]. Group 2 comprised patients who had hemihepatectomy without external bile drainage. Written informed consent was obtained from all study participants. The study protocol conformed to the ethical guidelines of the 1975 Declaration of Helsinki and was approved by the institutional review committee.

Hemihepatectomy was performed in a systematic manner in all patients. Patients with preoperative biliary drainage, previous cholecystectomy, bile duct excision or Child–Pugh grade B disease were excluded. During the study, the use of C-tube drainage was not absolutely required. Patients with no bile leakage from the cutting surface and no bile duct injury were mainly assigned to the no C-tube drainage group. The chief surgeon decided whether to use the C tube.

In all patients, serum bile acid levels were measured before, and 1, 3, 7 and 14 days after hemihepatectomy. Serum samples were collected early in the morning after overnight fasting. Oral intake was permitted from the day after hepatic resection. Serum bile acid levels, indocyanine green retention rate at 15 min and total bilirubin levels were measured using a liquid-stable enzymatic colorimetric assay, fluorescence assay and 2,5-dichlorophenyldiazonium assay respectively. Liver transection was performed by an ultrasonic surgical aspirator with precoagulation technique and liver hanging manoeuvre[10]. The number of Pringle manoeuvres applied (15 min of clamping and 5 min of release) was kept to a minimum. The amount of blood loss was calculated from blood in suction devices and gauze weight. The Child–Pugh classification was used to assess liver function.

Liver volumetry

Computed tomography (CT) was performed in all patients within 7 days before surgery and at 7 days after hepatectomy. For volumetric analysis, axial images of the portal venous phase of contrast-enhanced CT and volumetry software, AZE VirtualPlace® (AZE, Chiyoda-ku, Tokyo, Japan), was used. The weight of the resected specimen was measured immediately after surgery on a balance. The density of the resected liver was considered to be approximately 1·0 g/ml[11]. The numerical value of volume of the resected specimen is normally approximately equal to the weight; therefore, volume was defined to be equal to weight. Remnant liver volume estimated immediately after hepatectomy was defined as the difference between the volume before hepatectomy and resected liver weight. The following volume parameters were defined: volume A (V_A), total liver volume before hepatectomy measured by CT volumetry; volume B (V_B), volume of the resected specimen; and volume C (V_C), liver volume calculated by CT volumetry on day 7 after hepatectomy. Regenerated liver volume was calculated as $V_C - (V_A - V_B)$ and percentage liver regeneration was calculated as 100 per cent $\times [V_C - (V_A - V_B)]/(V_A - V_B)$.

Statistical analysis

Baseline data are presented as mean(s.d.). Data for the different groups and categorical data were compared using unpaired t tests and χ^2 test respectively. The unpaired two-group t test was used to evaluate changes in remnant liver volume after hepatectomy. Pearson's correlation was used to perform simple linear regression to study the association between increases in liver regeneration volumes and rates and serum bile acid levels. All significance tests were two-sided, and $P < 0{\cdot}050$ was considered to be statistically significant. The statistical software package SPSS® Statistics for Windows® version 18·0·0 (IBM, Chicago, Illinois, USA) was used for statistical analysis.

Results

A total of 409 partial hepatectomies were performed at the authors' institution during the study period. Seventy-nine consecutive patients underwent (extended) hemihepatectomy and 46 of these were included in the study. Patients who had a previous PVE (6 patients), combined hepatectomy or radiofrequency ablation (7), synchronous

resection of other organs (6), bile duct reconstruction (2), accompanying macroscopic portal vein tumour thrombus (2) and insufficient perioperative data/diagnostic images (10) were excluded. There were 35 men and 11 women of mean age 65(12) (range 35–84) years; 24 patients had a right-sided hemihepatectomy (6 extended) and 22 a left-sided major hemihepatectomy (8 extended). Primary diagnoses included hepatocellular carcinoma (24), intrahepatic cholangiocarcinoma (8), colorectal liver metastases (8) and other condition (6). Twenty-nine patients were included in group 1 and 17 in group 2. C-tube drainage was avoided because of previous cholecystectomy in five patients, difficulties in insertion in five, no cholecystectomy in one patient and surgeon decision in six patients.

Perioperative findings

Age, sex, liver function, duration of surgery, amount of intraoperative blood loss and frequency of blood transfusion were similar in the two groups (*Table 1*). The estimated total and resected liver volumes were equivalent. According to the new Inuyama classification[12], the extent of liver fibrosis and necroinflammatory activity was similar. Morbidity equal to or greater than grade III, assessed according to the Clavien–Dindo classification[13], was comparable between the groups. Biliary leakage defined as grade III[13] was encountered in one patient in group 1 and one in group 2.

Serum bile acid levels before and after hepatectomy

The median duration of biliary drainage was 10 days (*Table 1*). Mean serum bile acid levels before and on days 1, 3, 7 and 14 after hepatectomy were 12·2(9·9), 3·7(6·7), 2·7(2·1), 5·5(4·0) and 14·1(18·7) μmol/l in group 1, and 9·9(7·6), 2·8(1·6), 11·6(13·5), 17·6(15·0) and 16·7(9·8) μmol/l in group 2 respectively. There was no difference in serum bile acid levels between the two groups before hepatectomy. Serum bile acid levels on days 3 and 7 after hepatectomy were significantly higher in group 2 than in group 1 (*Fig. 1*). Subgroup analysis revealed that serum bile acid levels were similar in the 22 patients who underwent left-sided hepatectomy and the 24 patients who had right-sided hepatectomy. Mean levels on day 3 after hepatectomy in group 1 were 2·8(1·9) and 2·5(2·7) μmol/l for the left- and right-sided groups respectively, and those in group 2 were 12·2(16·0) and 14·3(13·2) μmol/l. These differences had disappeared after cessation of external biliary drainage on day 14 after hepatectomy.

Liver regeneration after hepatectomy

In the 46 patients who underwent hemihepatectomy, liver regeneration volumes on day 7 after surgery were significantly higher in group 2 than in group 1; mean regenerated liver volume was 40·0(158·8) (range from −147 to 226) ml

Table 1 Comparison of perioperative characteristics in 46 patients undergoing major hepatectomy with (group 1) and without (group 2) bile drainage

	Drainage ($n = 29$)	No Drainage ($n = 17$)	P‡
Age (years)*	66(13)	64(11)	0·664
Sex ratio (M : F)	20 : 9	15 : 2	0·139§
$ICGR_{15}$ (%)*	12·7(7·6)	12·2(5·6)	0·833
Child–Pugh grade			1·000§
A	29	17	
B	0	0	
Total bilirubin before hepatectomy (mg/dl)*	0·74(0·29)	0·78(0·18)	0·621
Total liver volume before hepatectomy (ml)*	1294(535)	1390(708)	0·607
Duration of surgery (min)*	431(80)	409(108)	0·441
Intraoperative bleeding (ml)*	503(507)	339(249)	0·221
Blood transfusion	4	0	0·109§
Resected liver weight (g)*	558(404)	624(657)	0·676
F stage†			0·972§
0–2	24	14	
3–4	5	3	
A grade†			0·683§
0–1	17	11	
2–3	12	6	
Complications (Clavien–Dindo grade > III)	5	2	0·618§
Median duration of biliary drainage (days)	10	–	0·002

*Values are mean(s.d.). †The extent of liver fibrosis (F stage) and necroinflammatory activity (A grade) were classified according to the new Inuyama classification[12]. $ICGR_{15}$, indocyanine green retention rate at 15 min. ‡Unpaired t test, except §χ^2 test.

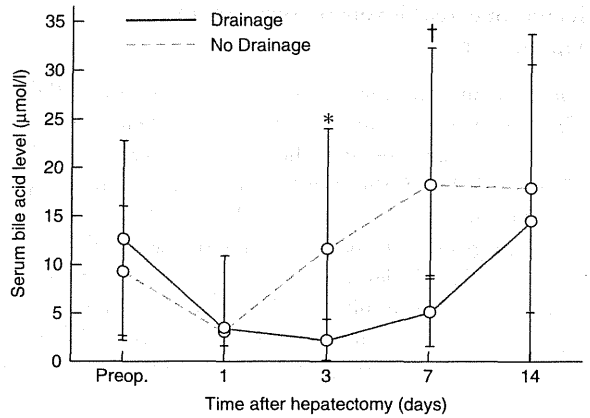

Fig. 1 Changes in mean serum bile acid levels after major hepatectomy in 46 patients undergoing hepatectomy with (group 1) and without (group 2) bile drainage. *$P = 0{\cdot}003$, †$P = 0{\cdot}022$ (unpaired t test)

in group 1 and 138·1(135·9) (−38 to 385) ml in group 2 ($P = 0{\cdot}038$). Mean percentage remnant liver regeneration was 11·0(24·7) (range from −14·1 to 42·3) per cent in group 1 and 22·5(27·6) (−4·3 to 103·5) per cent in group 2 ($P = 0{\cdot}158$). Subgroup analysis of the 22 patients who had a left-sided hemihepatectomy revealed that mean liver regeneration volume on day 7 after surgery was significantly higher in group 2: 149·6(78·6) ml *versus* 24·0(101·5) ml in group 1 ($P = 0{\cdot}018$). In line with this, liver regeneration rates for the remnant liver were significantly higher in group 2 than in group 1 (29·1(16·9) *versus* 3·4(13·1) per cent respectively; $P = 0{\cdot}001$). In the 24 patients who underwent a right-sided hemihepatectomy, mean liver regeneration volumes on day 7 after surgery were significantly higher in group 2 (211·1(140·7) ml *versus* 57·5(149·9) ml in group 1; $P = 0{\cdot}026$). Liver regeneration rates for the remnant liver after right hemihepatectomy were not significantly higher in group 2 (37·6(33·1) *versus* 12·1(25·5) per cent; $P = 0{\cdot}052$).

Association between serum bile acid levels and liver regeneration

The data obtained on day 3 after hepatectomy were selected to predict the extent of liver regeneration as early as possible. Liver regeneration rates on day 7 after hepatectomy showed a significant positive association with serum bile acid levels on day 3 after hepatectomy in the 46 patients included in the study; however, no significant association was observed between regeneration rates on day 7 after hepatectomy and serum bile acid levels on day 1 or 7. Liver regeneration volumes on day 7 after hepatectomy showed a significant positive association with serum bile

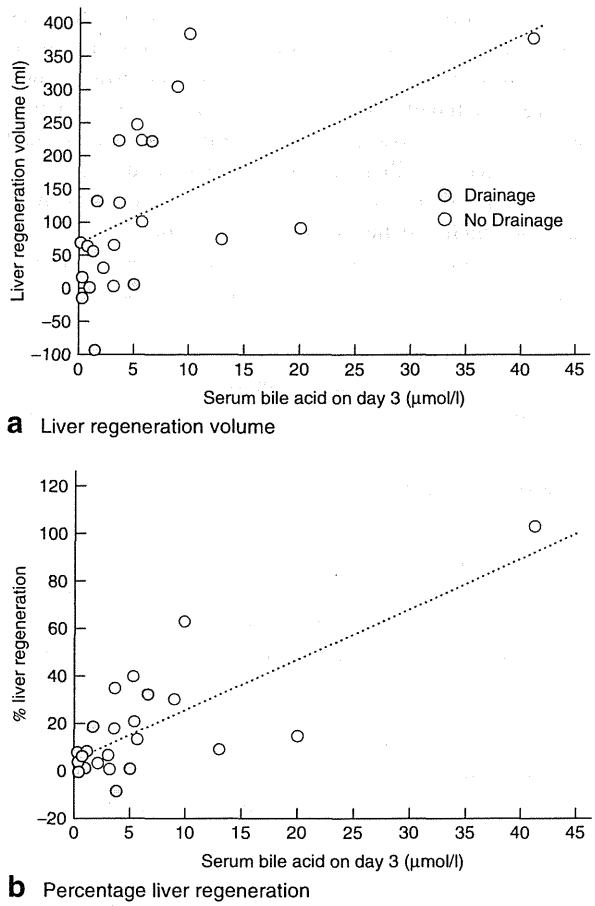

Fig. 2 Association between liver regeneration on day 7 and serum bile acid levels measured on day 3 in patients undergoing major hepatectomy with (group 1, $n = 11$) and without (group 2, $n = 14$) bile drainage: **a** liver regeneration volume; **b** percentage liver regeneration

acid levels on day 3 after hepatectomy. Liver regeneration volumes on day 7 after hepatectomy could be predicted using the formula 68·664 + 7·83× serum bile acid level on day 3 ($R = 0{\cdot}55$, $P = 0{\cdot}006$) (*Fig. 2a*). Similarly, liver regeneration rates on day 7 after hepatectomy showed a significant positive association with serum bile acid levels on day 3 after hepatectomy. Liver regeneration rates on day 7 after hepatectomy were calculated using the equation 4·81 + 2·124 × serum bile acid level on day 3 ($R = 0{\cdot}76$, $P < 0{\cdot}001$) (*Fig. 2b*).

Discussion

In this study, major hepatectomy induced an increase in serum bile acid levels that was more marked among patients

who showed the greatest hypertrophy of the liver. Biliary drainage with a C tube has sometimes been applied to reduce the risk of biliary leakage after hepatectomy[10] and is useful to obtain bile juice for evaluation of liver function[14]. The rate of complications, including biliary leakage, in patients who underwent major hepatectomy with biliary drainage in the present study was similar to that in patients without biliary drainage. In addition, these results clearly demonstrate that external biliary drainage not only caused a significant decrease in serum bile acid levels but also was associated with significantly worse liver regeneration after major hepatectomy. In partially hepatectomized rats, preoperative external biliary drainage leads to loss of bile acid and results in delayed liver regeneration after partial hepatectomy compared with rats with internal biliary drainage[6–8]. The absence of bile acids in the intestine after hepatectomy apparently delays liver regeneration and this may be associated with cyclin E-associated kinase inactivation[8].

In rodent models of 70 per cent partial hepatectomy, bile acid feeding stimulates liver hypertrophy and the rate of liver growth by proliferation of hepatocytes[3]. Bile acids are products of cholesterol catabolism that are synthesized in the liver and secreted into the intestine via the bile duct after food intake. Most of the bile acids are reabsorbed from the intestine and transported back to the liver through the portal vein. External drainage of bile juice at least partially interrupts this enterohepatic circulation. Activation of FXR is required for normal liver regeneration[3]. FXR is a nuclear receptor that recognizes bile acids as endogenous ligands[15]. This receptor plays an important role in mediating crosstalk between the liver and intestine to maintain bile acid, lipid and glucose homeostasis. FXR-knockout mice develop cholestasis, gallstones, non-alcoholic fatty liver disease, carcinogenesis in the liver and systemic metabolic abnormalities[16–19]. The absence of FXR stimulation in the ileum, with less fibroblast growth factor (FGF) 19 production and transport to the liver subsequently, may lead to less hepatic FGF receptor 4 production, which results in increased cytochrome P450 7A1 (CYP7A1) production. Raised levels of CYP7A1 may increase production of bile acids from cholesterol and lead to increased bile acid release into the cholangiocytes[3–5]. As serum concentrations of bile acids were lower in the drained patients, it may be postulated that the extra bile acids produced were drained externally.

Patients who underwent PVE before hepatectomy were excluded from this study. In PVE-treated patients undergoing hepatectomy, liver regeneration follows a two-stage pattern. After PVE, the non-embolized lobe regenerates and subsequently, after major hepatectomy, liver regeneration again occurs but to a lesser extent than that in patients without PVE undergoing a similar liver resection[20]. This study demonstrated that serum bile acid levels on day 3 after hepatectomy were associated with liver regeneration rates and volumes on day 7 after hepatectomy. In support of this, it was previously reported that increases in serum bile acid levels on day 3 after right PVE were strongly associated with effective hypertrophy of the non-embolized liver after PVE[9]. Bile acids are toxic, and increases in hepatic bile acid levels can induce both apoptosis and necrosis of hepatocytes[21]. Bile acid levels in hepatocytes should thus be tightly regulated to prevent cell damage[22] or liver fibrosis[23]. Increased bile acid levels immediately after hepatectomy or PVE may indicate decreased functional capacity of the liver and induce liver regeneration via FXR activation to prevent cell damage. In humans, effective hypertrophy of the remnant liver after hepatectomy and in non-embolized liver after PVE could possibly be evaluated on the basis of serum bile acid levels on day 3. This provides earlier information than increases in transforming growth factor α, serum hepatocyte growth factor and transforming growth factor β1 levels on day 14[24,25].

Disclosure

The authors declare no conflict of interest.

References

1 Buell JF, Rosen S, Yoshida A, Labow D, Limsrichamrern S, Cronin DC *et al.* Hepatic resection: effective treatment for primary and secondary tumors. *Surgery* 2000; **128**: 686–693.

2 Shiratori Y, Shiina S, Imamura M, Kato N, Kanai F, Okudaira T *et al.* Characteristic difference of hepatocellular carcinoma between hepatitis B- and C- viral infection in Japan. *Hepatology* 1995; **22**: 1027–1033.

3 Huang W, Ma K, Zhang J, Qatanani M, Cuvillier J, Liu J *et al.* Nuclear receptor-dependent bile acid signaling is required for normal liver regeneration. *Science* 2006; **312**: 233–236.

4 Xing X, Burgermeister E, Geisler F, Einwächter H, Fan L, Hiber M *et al.* Hematopoietically expressed homeobox is a target gene of farnesoid X receptor in chenodeoxycholic acid-induced liver hypertrophy. *Hepatology* 2009; **49**: 979–988.

5 Zhang L, Huang X, Meng Z, Dong B, Shiah S, Moore DD *et al.* Significance and mechanism of CYP7a1 gene regulation during the acute phase of liver regeneration. *Mol Endocrinol* 2009; **23**: 137–145.

6 Suzuki H, Iyomasa S, Nimura Y, Yoshida S. Internal biliary drainage, unlike external drainage, does not suppress the

regeneration of cholestatic rat liver after partial hepatectomy. *Hepatology* 1994; **20**: 1318–1322.
7 Saiki S, Chijiiwa K, Komura M, Yamaguchi K, Kuroki S, Tanaka M. Preoperative internal biliary drainage is superior to external biliary drainage in liver regeneration and function after hepatectomy in obstructive jaundiced rats. *Ann Surg* 1999; **230**: 655–662.
8 Ueda J, Chijiiwa K, Nakano K, Zhao G, Tanaka M. Lack of intestinal bile results in delayed liver regeneration of normal rat liver after hepatectomy accompanied by impaired cyclin E-associated kinase activity. *Surgery* 2002; **131**: 564–573.
9 Hayashi H, Beppu T, Sugita H, Horino K, Komori H, Masuda T *et al.* Increase in the serum bile acid level predicts the effective hypertrophy of the nonembolized hepatic lobe after right portal vein embolization. *World J Surg* 2009; **33**: 1933–1940.
10 Beppu T, Ishiko T, Chikamoto A, Komori H, Masuda T, Hayashi H *et al.* Liver hanging maneuver decreases blood loss and operative time in a right-side hepatectomy. *Hepatogastroenterology* 2012; **59**: 542–545.
11 Karlo C, Reiner CS, Stolzmann P, Breitenstein S, Marincek B, Weishaupt D *et al.* CT- and MRI-based volumetry of resected liver specimen: comparison to intraoperative volume and weight measurements and calculation of conversion factors. *Eur J Radiol* 2009; **75**: 107–111.
12 Ichida F, Tsuji T, Omata M. New Inuyama Classification; new criteria for histological assessment of chronic hepatitis. *Int Hepatol Commun* 1996; **6**: 112–119.
13 Clavien PA, Barkun J, de Oliveira ML, Vauthey JN, Dindo D, Schulick RD *et al.* The Clavien–Dindo classification of surgical complications: five-year experience. *Ann Surg* 2009; **250**: 187–196.
14 Hotta T, Kobayashi Y, Taniguchi K, Johata K, Sahara M, Ochiai M *et al.* Liver functional analysis by total bile acid level of C-tube bile after hepatectomy. *Hepatogastroenterology* 2005; **52**: 1211–1215.
15 Parks DJ, Blanchard SG, Bledsoe RK, Chandra G, Consler TG, Kliewer SA *et al.* Bile acids: natural ligands for an orphan nuclear receptor. *Science* 1999; **284**: 1365–1368.
16 Moschetta A, Bookout AL, Mangelsdorf DJ. Prevention of cholesterol gallstone disease by FXR agonists in a mouse model. *Nat Med* 2004; **10**: 1352–1358.
17 Guo GL, Santamarina-Fojo S, Akiyama TE, Amar MJA, Paigen BJ, Brewer B Jr *et al.* Effects of FXR in foam-cell formation and atherosclerosis development. *Biochim Biophys Acta* 2006; **1761**: 1401–1409.
18 Yang F, Huang X, Yi T, Yen Y, Moore DD, Huang W. Spontaneous development of liver tumors in the absence of the bile acid receptor farnesoid X receptor. *Cancer Res* 2007; **67**: 863–867.
19 Kong B, Luyendyk JP, Tawfik O, Guo GL. Farnesoid X receptor deficiency induces nonalcoholic steatohepatitis in low-density lipoprotein receptor-knockout mice fed a high-fat diet. *J Pharmacol Exp Ther* 2009; **328**: 116–122.
20 van den Esschert JW, de Graaf W, van Lienden KP, Busch OR, Heger M, van Delden OM *et al.* Volumetric and functional recovery of the remnant liver after major liver resection with prior portal vein embolization: recovery after PVE and liver resection. *J Gastrointest Surg* 2009; **13**: 1464–1469.
21 Kullak-Ublick GA, Meier PJ. Mechanisms of cholestasis. *Clin Liver Dis* 2000; **4**: 357–385.
22 Chiang JY. Bile acid regulation of gene expression: roles of nuclear hormone receptors. *Endocr Rev* 2002; **23**: 443–463.
23 Fiorucci S, Antonelli E, Rizzo G, Renga B, Mencarelli A, Riccardi L *et al.* The nuclear receptor SHP mediates inhibition of hepatic stellate cells by FXR and protects against liver fibrosis. *Gastroenterology* 2004; **127**: 1497–1512.
24 Kusaka K, Imamura H, Tomiya T, Makuuchi M. Factors affecting liver regeneration after right portal vein embolization. *Hepatogastroenterology* 2004; **51**: 532–535.
25 Hayashi H, Beppu T, Sugita H, Masuda T, Okabe H, Takamori H *et al.* Serum HGF and TGF-beta1 levels after right portal vein embolization. *Hepatol Res* 2010; **40**: 311–317.

Surg Today
DOI 10.1007/s00595-012-0371-x

HOW TO DO IT

End-to-side pancreaticojejunostomy without stitches in the pancreatic stump

Daisuke Hashimoto · Masahiko Hirota · Yasushi Yagi · Hideo Baba

Received: 30 March 2012 / Accepted: 5 July 2012

Abstract In patients undergoing pancreaticoduodenectomy, leakage from the pancreatic anastomosis remains an important cause of morbidity and contributes to prolonged hospitalization and mortality. Recently, a new end-to-end pancreaticojejunostomy technique without the use of any stitches through the pancreatic texture or pancreatic duct has been developed. In this novel anastomosis technique, the pancreatic stump is first sunk into deeply and tightened with a purse string in the bowel serosa. We modified this method in an end-to-side manner to complete the insertion of the pancreatic stump into the jejunum, independent of the size of the pancreas or the jejunum. We tested this new anastomosis technique in four pilot patients and compared their outcomes with four control patients who underwent traditional pancreaticojejunostomy. No severe pancreatic fistulas were observed in either group. There were no differences in morbidity or hospital stay between the groups. This new method can be performed safely and is expected to minimize leakage from pancreaticojejunostomies.

Keywords Pancreaticoduodenectomy · Pancreaticojejunostomy · Pancreatic fistula

D. Hashimoto · H. Baba (✉)
Department of Gastroenterological Surgery, Kumamoto University Graduate School of Medical Sciences,
1-1-1 Honjo, Kumamoto 860-8556, Japan
e-mail: hdobaba@kumamoto-u.ac.jp

D. Hashimoto · M. Hirota · Y. Yagi
Department of Surgery, Kumamoto Regional Medical Center,
5-16-10 Honjo, Kumamoto 860-0811, Japan

Introduction

Problems with pancreaticojejunostomies and pancreaticogastrostomy anastomoses are the main causes of early morbidity after pancreaticoduodenectomy (PD) [1–5]. Therefore, this study focused on generating a method for anastomosing the pancreas with the jejunum that might reduce the rate of complications associated with this difficult type of anastomosis.

Recently, it was found that postoperative pancreatic fistula (POPF) may mediate many of the complications observed after pancreatic resection [6]. Several authors have previously reported that a soft pancreatic texture constitutes a major risk factor for postoperative complications, including POPF [7, 8].

The pancreas is extremely vulnerable to handle. The use of surgical scalpels, instead of electrocautery or ultrasonic techniques, may diminish trauma to the pancreatic stump induced by resection [9]. In addition, using a thin suture material with as few stitches as possible and avoiding any excessive tightening of the sutures have been reported to reduce injury to the pancreas in rats [9]. In general, multiple stitches are used to secure the anastomosis between the pancreas and the jejunum or stomach, regardless of the type of reconstruction used. In order to minimize pancreatic injury induced by multiple stitches, a novel anastomosis technique has been developed [10] in which the pancreatic stump is inserted into the jejunum deeply in an end-to-end fashion and tightened with a purse string in the jejunal serosa without the use of any stitches through the pancreatic texture or pancreatic duct [10]. This technique may not be completed if the intestines are too small or the pancreatic stump is too large to insert the pancreatic stump into the jejunum. We modified this method in an end-to-side manner to complete the insertion of the pancreatic stump into the jejunum, independent of the size of the pancreas or the jejunum.

Published online: 11 October 2012

Patients and methods

PD surgical technique

PD was performed with D2 dissection of the lymph nodes [11–13]. There were no patients with possible portal/superior mesenteric vein invasion. In each case, the neck of the pancreas was transected using a surgical scalpel. Artificial bleeding on the side of pancreatic stump was controlled with precisely positioned monofilament sutures, and smaller areas of bleeding were treated with compression. The jejunum was cut, and the cut end of the anal side was moved up retrocolically through the incision in the right side of the transverse mesocolon. Pancreaticojejunostomy was performed in two ways, as described below, and a non-absorbable stent tube was inserted into the main pancreatic duct to avoid obstruction. Hepaticojejunostomy and gastrojejunostomy were performed distal to the pancreaticojejunostomy.

Surgical technique of the new end-to-side pancreaticojejunostomy without stitches in the pancreatic stump

For reconstruction, an incision with the same diameter as the pancreatic stump was made on the opposite side of the mesenterium of the jejunum (Fig. 1a). The pancreatic stump was first isolated from the surrounding tissue with up to a 30-mm margin from the cut surface (Fig. 1b). It is necessary to insert the pancreatic remnant into the jejunum and to maintain a safe fixation between the pancreas and the jejunum. A purse string suture of absorbable 3-0 monofilament thread was applied around the incision of the jejunum (Fig. 1a). Four to five stay sutures of absorbable 4-0 monofilament thread were also applied around the pancreas (Fig. 1b). On the posterior side, stay sutures were applied on the peripancreatic retroperitoneal tissue carefully avoiding stitching the pancreatic parenchyma dissected from the splenic artery and vein, which should be completely covered by the jejunal wall. On the anterior side, stay sutures were applied on the serosa and parenchyma of the pancreas. The pancreatic stump was inserted into the jejunal incision in an end-to-side fashion applying the stay sutures on the incision to secure the depth of insertion (Fig. 1c, d). Finally, the purse string suture was tied to seal the anastomosis carefully avoiding the ischemia of the pancreatic stump. The stay sutures and the purse string sutures prevent the pancreatic stump from dropping out of the jejunum.

Surgical technique of traditional end-to-side pancreaticojejunostomy

Traditional pancreaticojejunostomy was also performed as end-to-side anastomosis. An incision of the jejunal wall proportional to the size of the pancreatic duct was created. Eight to 10 sutures of 4-0 monofilament thread were applied taking the pancreatic duct and the whole pancreatic parenchyma, followed by taking the whole layer of the jejunum, enough to cover the pancreatic stump. After being placed, all sutures were tied.

Patients and POPF

Between 2009 and 2011, eight patients underwent PD at Kumamoto Regional Medical Center. All procedures were performed by one surgeon. Written informed consent was obtained before surgery. Pancreaticojejunostomy was performed using the new method in four pilot patients and using the traditional method in four patients. We evaluated patient backgrounds, operative times, operative bleeding, pancreatic textures and outcomes after surgery. The incidence of POPF was assessed according to the International Study Group (ISGPF) definition [14]. Grade A was excluded from postoperative complications because it had no clinical impact.

Statistical analysis

The median test and the Chi square test were used to evaluate differences in each parameter. A P value < 0.05 was considered to be statistically significant.

Results

The patient characteristics are listed in Table 1. There were no significant differences in age or sex ratios. The pancreatic textures were soft in three of the patients in the new method group and two patients in the traditional method group. The operative parameters and outcomes after surgery are listed in Table 2. There were no significant differences in operative time, bleeding or length of hospital stay after surgery. Delayed gastric empting (DGE) was observed in only one patient in the new method group. Although one patient in the traditional method group developed grade A POPF, there were no hospital deaths or patients with grade B or C POPF in either group.

Discussion

Although PD has been performed safely in high volume centers, mortality and morbidity remain high, and the procedure is largely associated with problems during pancreatic reconstruction [1–4]. In order to minimize surgical damage to the cut end of the pancreas and to cover it completely with the jejunal wall, Nordback et al. [10]